Available online at www.sciencedirect.com
SCIENCE DIRECT
Biochimica et Biophysica Acta 1710 (2005) 67 – 77
BIOCHIMICA ET BIOPHYSICA ACTA
BBA
http://www.elsevier.com/locate/bba

Application of classical molecular dynamics for evaluation of proton transfer mechanism on a protein

Ran Friedman, Esther Nachliel, Menachem Gutman *

Laser Laboratory for Fast Reactions in Biology, Department of Biochemistry, The George S. Wise Faculty for Life Sciences, Tel Aviv University, Ramat Aviv, 69978 Tel Aviv, Israel

Received 5 April 2005; received in revised form 14 September 2005; accepted 16 September 2005
Available online 12 October 2005

Abstract

Proton transfer reactions on surfaces are prevalent in biology, chemistry and physics. In the present study, we employed classical Molecular Dynamics simulations to search for the presence of transient configurations that enable proton transfer, or proton sharing, between adjacent carboxylate groups on the protein surface. The results demonstrate that, during random fluctuations of the residues on the surface, there are repeated situations in which nearby carboxylates either share a common proton through a hydrogen bond, or are connected by a few water molecules that form conducting networks. These networks do not extend out of the common Coulomb cage of the participating residues and the lifetimes of the bridged structures are sufficiently long to allow passage of a proton between the carboxylates. The detection of domains capable of supporting a rapid proton transfer on a protein supports the notion that clusters of carboxylates are the operative elements of proton collecting antennae, as in bacteriorhodopsin, cytochrome *c* oxidase or the photosynthetic reaction center.

Keywords: Molecular dynamics; Proton transfer; Protein surface

1. Introduction

Proton transfer reactions on surfaces are tremendously important in biology, chemistry and physics. Membrane-bound proton-pumping proteins such as bacteriorhodopsin, cytochrome *c* oxidase and the photosynthesis reaction center utilize proton-collecting antennae, which collect protons from the surrounding media and channel them to the proton transfer channels [1–5]. Membrane structures, as well as polymers like nafion, can also form a scaffold for proton-transferring moieties [6–11].

Proton transfer on surfaces can either proceed directly from a donor to an acceptor, or indirectly via interconnecting water molecules that form a proton conducting network between the donor and acceptor moieties. We shall refer to the first mechanism as *direct proton transfer*, while the second mechanism will be referred to as *solvent mediated proton transfer*. If two moieties (e.g., carboxylic amino acids) have similar pK_as and are hydrogen-bonded through a short, strong hydrogen bond, they effectively share a proton between them until the hydrogen bond breaks and the proton will become associated with a single group. Thus, proton sharing among two such groups can be referred to as direct proton transfer, when the hydrogen bond finally breaks. The sharing of a proton between two sites can be detectable as a continuum adsorption band in the infrared spectrum [12]. Pairs of protein residues that allow direct proton transfer in such a mechanism can be found in a plethora of protein structures [13,14].

Solvent mediated proton transfer can be efficient in close compartments, as in the case of the carbonic anhydrase protein [15,16]; or when the donor and acceptor are surrounded by a common Coloumb cage [17,18]. The efficiency of the proton transfer under these conditions depends on the length of the proton transfer path and on the dimensions of the Coulomb cage. The reaction can be highly efficient when the donor and the acceptor are close enough for their solvation shells to be united, or when the number of interconnecting water molecules is small enough to enable their location beneath the surrounding

Abbreviations: CPMD, Car-Parrinello Molecular Dynmics; MD, Molecular Dynamics; PDB, Protein Data Bank; RMSD, Root Mean Square Deviation

* Corresponding author.
E-mail address: me@hemi.tau.ac.il (M. Gutman).

0005-2728/$ - see front matter © 2005 Elsevier B.V. All rights reserved.
doi:10.1016/j.bbabio.2005.09.005

Coloumb cage [17,18]. In the latter case, the water molecules are ordered by the solute, and the negative electrostatic field favors the location of the proton near the proton binding moieties, rather than its diffusion to the bulk solvent.

Proton transfer on surfaces was previously measured using the Laser Induced Proton Pulse technique [5,17–21]. These studies suggested that proton transfer between sites anchored to a surface can proceed efficiently through relatively rare configurations that are randomly formed. It was argued that, although the probability for the formation of such configurations is low, once they are formed, they will conduct a rapid proton transfer. Thus, even relatively rare states can be effective in proton transfer machinery. A search for independent evidence of this assumption can be carried out using Molecular Dynamics (MD) simulations [18,22].

Simulations of proton transfer can be carried out using different levels of theory. These include quantum-mechanical simulation techniques (based on Car-Parrinello Molecular Dynmics, CPMD, reviewed in [23]), empirical valence bond and quantum mechanical/molecular mechanical simulations (both reviewed in [24]; see also [25]). These simulations are highly accurate, but computationally expensive and hence cannot be used to simulate proton transfer on the molecular surface. More recently, Lill and Helms developed a method called QHOP-MD, which allows the simulation of proton transfer events in classical (i.e., non quantum) MD simulations [26]. With the exception of the QHOP-MD method, classical MD simulations cannot be used to study proton-transfer reactions, as they do not allow the breaking and formation of bonds. On the other hand, classical MD simulations can readily simulate the formation of configurations that allow either direct or indirect proton transfer [27–29]. In the present study, we employ classical MD simulations to search for configurations that enable proton transfer or proton sharing between adjacent carboxyl groups on the protein surface. By the use of modern MD software, small proteins like the S6 ribosomal protein used in this study can be simulated for tens of nanoseconds. Thus, using MD, rare events that lead to proton transfer can be searched for. Due to computational limitations, such rare events cannot be studied by methods which are based on quantum chemistry (i.e., CPMD, EVB and QM/MM). QHOP-MD is also slower than conventional MD and is not widely available. Accordingly, we have used classical MD simulations.

The S6 ribosomal protein, which forms part of the bacterial 30S ribosomal central domain [30], is a globular protein of 101 amino acids, 32 of which are charged at a physiological pH (16 negative and 16 positive). The multiple abundance of negative residues makes it an excellent model for studies of events associated with proton transfer on the protein surface. In a previous study [31], it has been demonstrated that, due to the high density of charged residues and to the shape of the electrostatic field surrounding the S6, this protein can effectively detain ions on its surface. In the present study, we wish to use the S6 protein to test the hypothesis that carboxylate moieties generate structures suitable for rapid proton transfer between them through the random structural fluctuations.

Five independent, 10-ns-long MD simulations were performed in the current study. In the first run, all arginine and lysine residues were positively charged, while glutamate and aspartate residues were in their anionic state. In this simulation, we have followed the distances between pairs of carboxylates, which were less than 1 nm apart in the crystal structure of the protein (PDB code 1ris, [32]), in order to search for pairs which are close enough to allow proton transfer between them. Two pairs of carboxylate residues were found to be located close enough to have coinciding solvation shells throughout the simulation. These pairs were further examined to see if their charges were counter-balanced by positive residues during the simulation. This was the case for one of the pairs (glu38/glu66). The other pair (glu22/asp83) interacted mainly with the surrounding solvent. We therefore focused our attention on the pair glu22/asp83 as a model for the study of the events that lead to proton transfer reactions on the protein surface. A model system was constructed by protonation of one of the residues, glu22, and four independent MD simulations were run using different random seeds for the initial assignment of the atomic velocities. All four simulations were run with the proton on glu22 in order to gain a large sampling of equivalent protein structures.

During the simulations in which glu22 was protonated, we have analyzed the hydrogen bonds formed between glu22 and asp83. It was found that the residues formed hydrogen bonds, which lasted long enough to allow proton sharing (or direct proton transfer) among them during large fractions of the simulation time. On the other hand, nanosecond long periods at which glu22 and asp83 were not hydrogen-bonded were also evident during the simulations. This allowed the search for water networks that interconnected the donor and the acceptor. These networks were made of an average of 2–3 water molecules. The water molecules were located under the negative Coloumb cage umbrella, created by the negative residues of the protein. Accordingly, a proton ejected from the donor residue could proceed along the interconnecting water molecules towards the acceptor, with a low probability of being transferred to bulk waters. Our results demonstrate that both direct (proton sharing) and solvent-mediated proton transfer reactions should occur on the surface of the S6 ribosomal protein. The S6 is a globular protein which has no known function associated with proton transfer, and hence we consider this as evidence for the generality of the mechanism.

To the best of our knowledge, this is the first report in which classical MD simulations are used to study events that lead to proton transfer on the protein surface. As the formation of pairs of carboxylate oxygens that can share a proton is a rather frequent observation in protein crystal structures [14], our observations suggest that proton transfer events on protein surfaces are quite prevalent in nature. On the other hand, the establishment of proton-transfer pathways is itself a rare event, meaning that only a small number of all possible negative residues are able to form such pathways. Taking all the above into account, we conclude that the surface of proteins features both ion-binding [31] and proton transferring/sharing domains that can be effective in enzymatic catalysis, protein–solvent

interactions and even for the adsorption of ligands on the protein surface [33]. These domains are located on distinct regions and are not distributed uniformly on the protein surface. The detection of domains that enable rapid proton transfer on a protein supports the notion that clusters of carboxylates are the operative elements of proton collecting antennae as in bacteriorhodopsin, cytochrome *c* oxidase or the photosynthetic reaction center.

2. Methods

2.1. Molecular dynamics simulations

Five independent Molecular Dynamics simulations of the ribosomal protein S6 were performed as reported earlier [31]. In order to be consistent with chemical experiments and MD simulations which have been performed in our lab with the S6 Q16H/S17C double mutant, we have performed the simulations reported here using the same mutant protein. All simulations were performed using the Gromacs computer simulation software [34,35]. The arginine residues, lysine residues and N-terminus were protonated. The aspartate residues, glutamate residues and C-terminus were unprotonated, except for glu22, which was protonated in all but one of the simulations. The four simulations with protonated glu22 differed in the random assignment of the velocities prior to the simulations, which resulted in different starting configurations.

2.2. Geometry optimizations of a model for the interaction between glu22 and asp83

We have used *ab initio* geometry optimization in order to verify that the carboxylate groups glu22 and asp83 could remain in close contact in the absence of interactions with any positively charged residues or ions. The starting structure was obtained as follows. First, we screened the MD trajectory, looking for a configuration in which the distances between the carboxylate oxygens of glu22 and asp83 were smaller than 0.6 nm and the distances from the carboxylate oxygens of glu22 and asp83 to any positive residue or ion were larger than 0.6 nm. The minimal distances for the selected configuration are given in Table 1. For construction of the model, the coordinates of the carboxylate groups, the nearest carbon (CG for glu22, CB for asp83) and all the water molecules located within 0.35 nm of the carboxylate oxygens were extracted from the simulation trajectory. Three hydrogen atoms were added to the carbon atom near the carboxylate, thereby representing the amino acids as acetate ions. It should be mentioned that a similar model was used to study proton transfer interactions [36]. The final model (see Fig. 4) included 12 water molecules and a total of 50 atoms. The obtained structure was optimized by the GAMESS computer program [37], using Hartree Fock wave functions with the 6–31G* basis set. During the optimization, the coordinates of the CH_3 carbon atoms were fixed to their initial locations, allowing only the terminal groups to move. This was done in order to mimic the protein environment, where the residues are anchored to the protein backbone. All other atoms, including those of the water molecules, were allowed to move during the geometry optimization.

Table 1
The minimal distances between the carboxylate oxygens of glu83 and asp22 and selected groups (see text)

Group 1	Group 2	Minimal distance (nm)
glu22: carboxylate oxygens	asp83: carboxylate oxygens	0.39
glu22: carboxylate oxygens	Any hydrogen from a terminal group of arginine or lysine	0.78
glu22: carboxylate oxygens	Any Na^+ ion	2.84
asp83: carboxylate oxygens	Any hydrogen from a terminal group of arginine or lysine	0.86
asp83: carboxylate oxygens	Any Na^+ ion	3.04

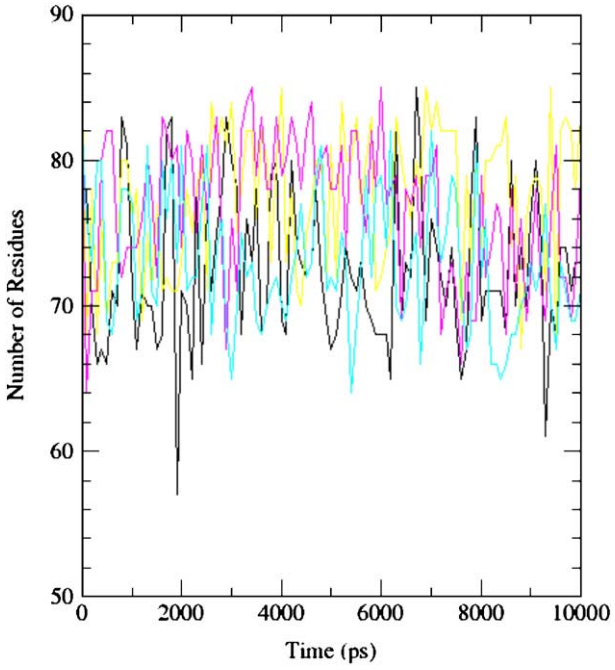

Fig. 1. The total number of amino acids, which form structural elements (α-helices, β-sheets, β-bridges and turns), calculated as a function of the simulation time for the four independent MD simulations of the S6 ribosomal protein mutant Q16H/S17C in which glu22 was protonated. Each simulation is shown in a different color. The total number of residues which form structural elements fluctuates around an average value of 72 to 77 amino acids (out of 97). There is no drift in the number of residues which form structural elements and the changes in the secondary structure elements are only temporary, thus indicating that the protein retains its secondary structure as the simulation runs. (For interpretation of the references to colour in this figure legend, the reader is referred to the web version of this article.)

2.3. Search for configurations that allow solvent-mediated proton transfer between glu22 and asp83

A 3-ns trajectory, during which no direct hydrogen bond bridged glu22 and asp83 (i.e., direct proton transfer between the residues was not possible during that period) was extracted from the simulation where glu22 was protonated. This trajectory was searched for the minimal number of water molecules that connected the donor and acceptor in each configuration. Two oxygen atoms (OE of glu22, OD of asp83 or water oxygens) were considered to be connected if the distance between them was smaller than 0.35 nm, as in [18]. The search for the interconnecting water networks was performed using home written software. In order to make the search both computationally efficient and comprehensive, it was performed on a subset of 100 structures, which were taken from the trajectory at 30 ps time intervals.

2.4. Structural analysis and visual presentation

The secondary structures of the simulated proteins were calculated using the computer program DSSP [38].

Illustrations of molecules were created using the VMD computer program [39], except for Fig. 4, which was created using the computer program molekel [40]. The electrostatic potential around the protein was calculated using the

computer program APBS [41], as previously described [31], under ionic strength of 50 mM.

3. Results and discussion

3.1. General structural and dynamics analysis

The S6 ribosomal protein functions as part of the bacterial ribosome [30]. The protein is stable in solution, and its structure was solved independently (i.e., not as a part of the ribosome) by X-ray crystallography [32,42]. The experience gained in our lab indicates that the Q16H/S17C double mutant is also stable at room temperature. Accordingly, the protein should be stable during MD simulations. This can be ascertained by means of a comparison of the backbone root mean square deviations (RMSD) relative to the crystal structure. In all simulations, the RMSDs did not exceed values of 0.238–0.299 nm (depending on the

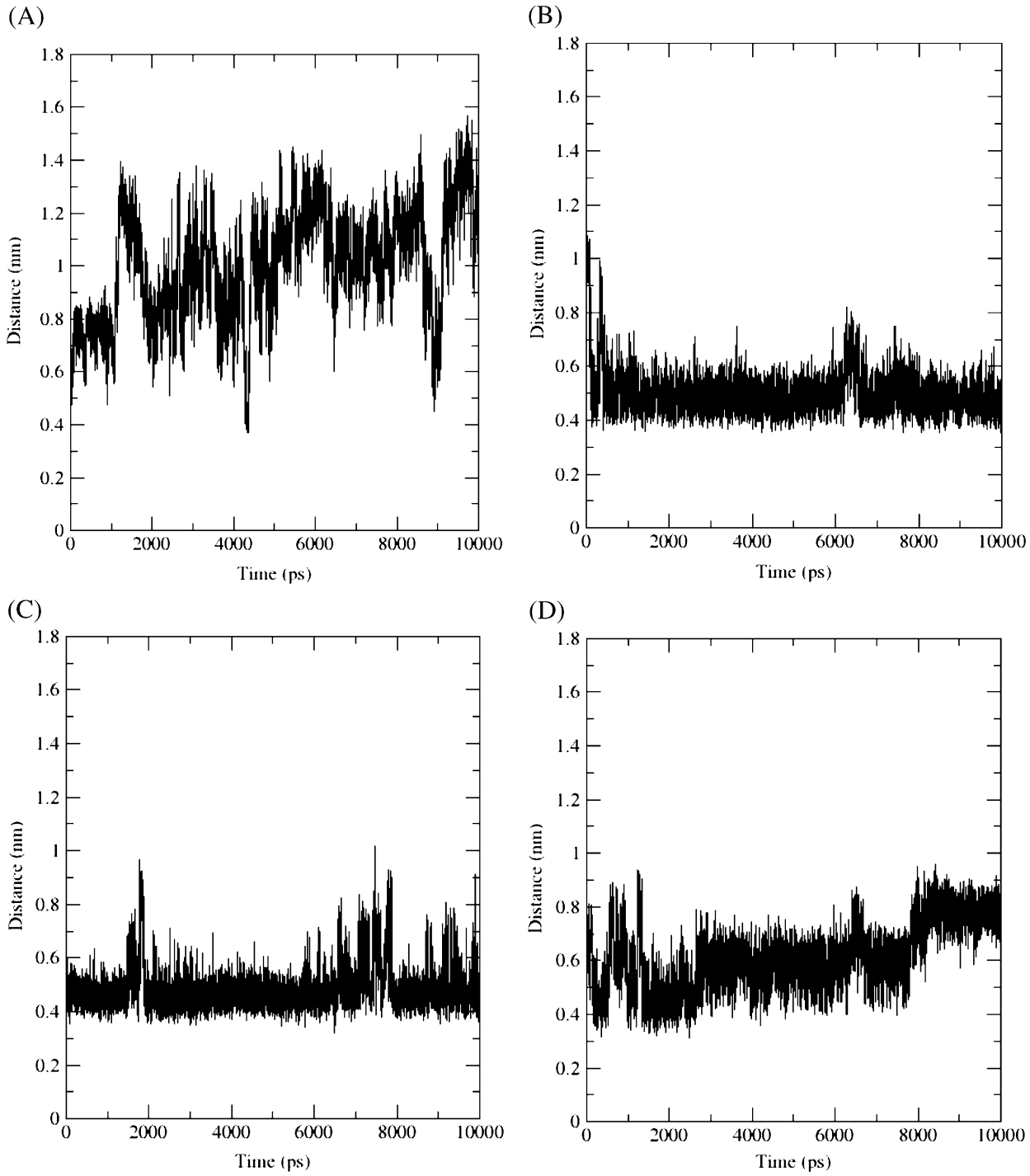

Fig. 2. The minimal distance between carboxylate oxygens of adjacent residues, as a function of simulation time. (A) glu5 and glu95; (B) glu22 and asp83; (C) glu38 and glu66; (D) glu 69 and asp70; (E) asp70 and asp74; (F) asp74 and glu78.

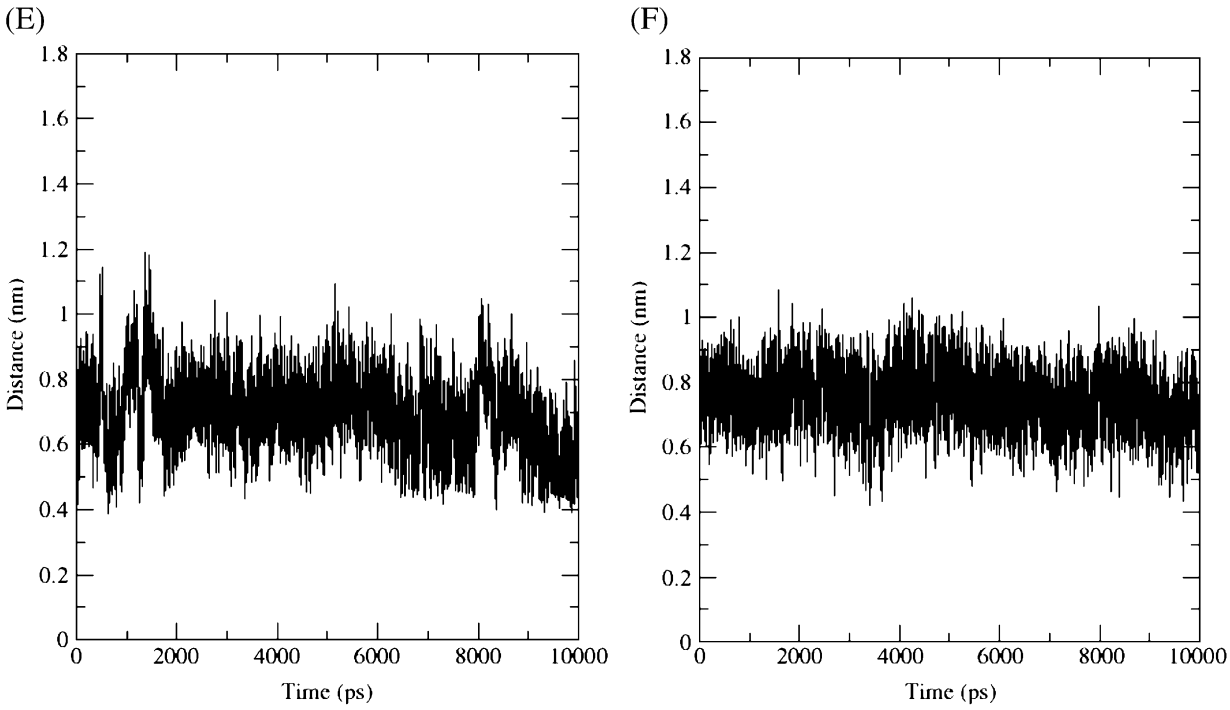

Fig. 2 (*continued*).

simulation), thus indicating that the protein is rather stable under the simulation conditions. Since we are interested in proton transfer between pairs of carboxylate residues, we have also examined the RMSD of the non backbone heavy atoms of the negative residues during the simulations. This group of atoms is more mobile than the protein's backbone, with RMSDs that reach maximal values of 0.382–0.438 nm.

In order to further validate the stability of the protein, the overall number of amino acids which formed structural elements (α-helices, β-sheets, β-bridges and turns) was calculated in the simulations in which glu22 was protonated. The results are presented in Fig. 1 (each color corresponds to a different simulation). The total number of residues which form structural elements fluctuates around an average value of 72 to 77 amino acids (out of 97). There is no drift in the number of residues which form structural elements, and the changes in the secondary structure are only temporary, which indicates that the protein retains its secondary structure as the simulation runs. Similar results were obtained for the simulation in which glu22 was negatively charged.

3.2. Contacts between the carboxylate oxygens in the simulation with all negative residues unprotonated

Direct proton transfer reactions on the protein surface demand that the solvation shells of the donor and acceptor overlap. Therefore, in order to locate configurations that will allow direct proton transfer (or proton sharing between two neighboring residues), we have followed the distances between the carboxylate oxygens of negative amino acid pairs which were located less than 1 nm apart in the crystal structure of the S6 (PDB code 1lou, [32]). The results are given in Fig. 2. The progress of the minimal distances between pairs of carboxylates reveals different trends. The distance may increase during the simulation (Fig. 2A). This variation is due to of the dissimilarity between the highly concentrated crystal liquor and the ionic solution in the simulation. In other cases, the distance may vary around an average value with some fluctuations (Fig. 2B, C, E, F) or show a transition between discrete states (Fig. 2D). The distance between the carboxylate oxygens was as small as ~0.5 nm in the case of the pairs glu22–asp83 and glu38–glu66 (Fig. 2B, C). This can make these dyads candidates for the study of proton transfer reactions on the protein surface, provided that this distance is comparable with the size of their first solvation shells.

In order to examine the size of the first solvation shells of the carboxylates, the radial distribution function of the water–oxygen to carboxylate–oxygen distance was calculated over the simulation trajectory. All of the carboxylate-bearing residues were included in the calculation. It was found that the radial distribution function had its first and most pronounced maximum at 0.28 nm. This maximum corresponds to the location of the first solvation shell of the carboxylate oxygen atoms. The average minimal distance between glu22 and asp83 (0.5 nm, Fig. 2B) and between glu38 and glu66 (0.49 nm, Fig. 2C) is smaller than twice the dimension of the solvation shell. Therefore, these pairs have common solvation shells and hence both glu22/asp83 and glu38/glu66 fulfill one of the most fundamental demands for proton transfer between adjacent residues [17].

3.3. The electrostatic interactions between pairs of carboxylates in the simulation with all glutamate and aspartate residues unprotonated

The electrostatic repulsion between two carboxylates drives the carboxylate moieties away from each other. This effect can be viewed, for example, in the case of the carboxylate oxygens of residues glu5 and glu95, which move apart during the simulation (Fig. 2A). However, other pairs of carboxylates, especially glu22/asp83 and glu38/glu66, stay in close contact throughout the simulation. This could occur due to neutralization of their charges by positive residues in their vicinity. To examine this, the minimal distances between the carboxylate oxygens of the pairs and the positively charged atoms (terminal hydrogens of amine- or guanido-groups and sodium ions) were calculated throughout the simulation. The minimal distance is the shortest of all distances to the two oxygen atoms. The results are presented in Fig. 3. An examination of the figure reveals that for the glu38/glu66 pair, the distances between the charged atoms are smaller than 0.3 nm throughout most of the simulation time, thus indicating that at least one residue of the pair glu38/glu66 is neutralized by means of a salt bridge throughout the simulation. Apparently, the positive charge facilitates the contact between the carboxylates.

The minimal distance between glu22/asp83 and the nearest positive atom (Fig. 3B) varies between a contact value of 0.18 nm and a maximal value of 0.93 nm. Throughout most of the simulation, these residues are not neutralized and are therefore likely to attract (and hold) a proton. Thus, the glu22/asp83 dyad can be used as a suitable model for the study of proton sharing among a pair of carboxylates or proton transfer on the protein surface. The other pair (flu38/glu66) does not form a good attractor for protons due to the presence of a positive charge in its vicinity.

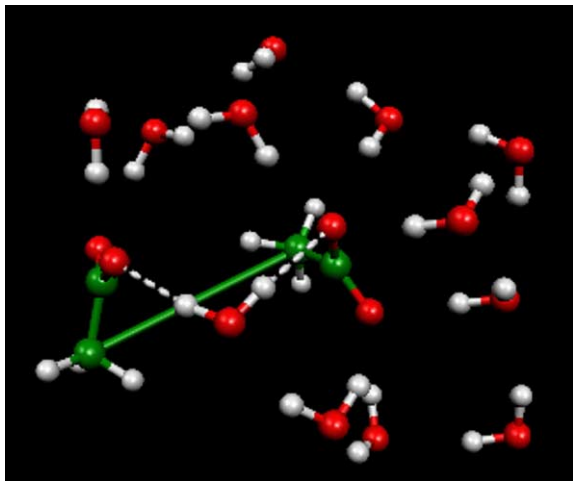

Fig. 4. The *ab initio* geometry optimized model for the glu22–asp83 interaction. The hydrogen bond between the carboxylate oxygens and the water molecule is depicted. Glu22:CG and asp83:CB are connected in the figure to signify that they were fixed during the geometry optimization.

3.4. The interactions between glu22, asp83 and the surrounding water

The carboxyles of glu22 and asp83 were held together during the simulation, without the aid of salt bridges with positive residues or Na^+ ions. It could be reasoned that the interaction between these residues can be mediated by the

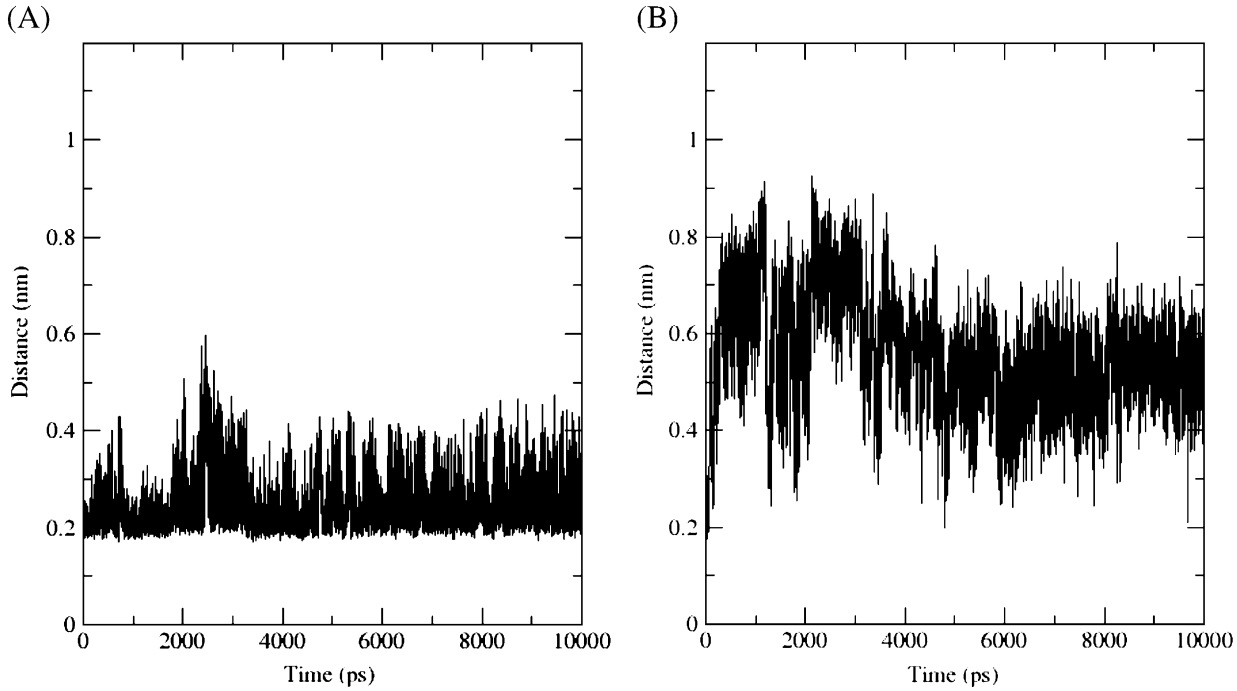

Fig. 3. The minimal distance between sodium ions or hydrogens from amino- or guanido-moieties and the carboxylate oxygens of (A) glu38/glu66 (B) glu22/asp83. The minimal distance is the shortest of all distances to the two oxygen atoms.

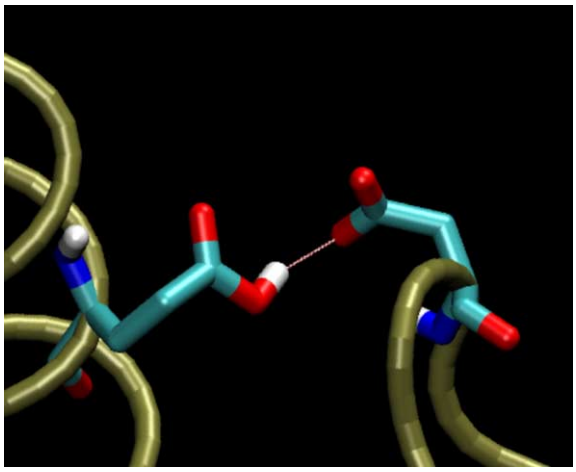

Fig. 5. The hydrogen bond created between the protonated glu22 and asp83 during the MD simulations.

solvent, as charged residues were previously found to strongly interact with the surrounding water [43,44]. By examining the interactions of glu22 and asp83 with the water, it was found that these residues formed hydrogen bonds with the solvent throughout 100% and 99.8% of the simulation time, respectively. Since both groups are highly solvated, we wished to check whether the solvent molecules fix the distance between them.

To account for the ability of the water to stabilize the connection of the two negatively charged carboxylates, we performed *ab initio* geometry optimization for the couple glu22–asp83. The residues were modeled as acetate ions, since use of the complete structure of the amino acids would make the calculation computationally prohibitive. The model structure included the carboxylate groups, the nearest carbon atoms (CG for glu22, CB for asp83) and the water molecules located within a distance of 0.35 nm of the carboxylate oxygen atoms. Following the geometry optimization, the distance between the oxygens is expected to grow, due to the strong electrostatic repulsion between the carboxylate species. This distance can be expected to be dictated by the constraint that distance between glu22:CD and asp83:CG is fixed at 0.511 nm (all other atoms, including those of the water molecules, were allowed to move). Therefore, the maximal distance between glu22:OE–asp83:OD should be around 0.8 nm. Surprisingly, after geometry optimization, the separation was only 0.44 nm. Fig. 4 presents the optimized structure. As seen in the figure, the two carboxylates are connected through a hydrogen-bonding water molecule, which bridges them and masks the repulsive electrostatic interactions. In the fully solvated system, it is common to find more than a single water molecule between asp22 and glu83, but the residues maintain close contact. The *ab initio* calculation points to the possibility that a structure, which contains two negative residues in close proximity, can be stable despite the electrostatic repulsion. Apparently, the stability can be gained not only by neutralizing the negative charges (as in the pair glu38/glu66) but also through hydrogen bonding water molecules (in glu22/asp83).

3.5. Hydrogen bonds in the simulations with protonated glu22

To further examine events that are involved in proton transfer on the protein surface, we have run four independent 10 ns long MD simulations with protonated glu22. The simulations differed in the initial (random) assignment of atomic velocities prior to the position-restrained and equilibration runs. In these simulations, we were able to search for configurations that would allow either a direct proton transfer between glu22 and asp83 or proton transfer through interconnecting water molecules.

To search for conditions that would allow direct proton transfer on the protein surface (or proton sharing through a common hydrogen bond), the number of hydrogen bonds between the hydroxyl moiety attached to glu22:CD and the carboxylate moiety of asp83 was followed during the simulations. Direct hydrogen bonds between the protonated glu22 and asp83 (as shown in Fig. 5) were evident in all simulations. The time fraction at which these residues were hydrogen bonded to each other varied from 15% to 61%, as summarized in Table 2.

The time scale for proton transfer in strongly hydrogen-bonded systems such as H_3O^+–H_2O and $NH4^+$–H_2O in vacuo is 10–40 [45]. During the MD simulations, the lifetimes of the hydrogen bonds between glu22 and asp83 are in the order of tens of picoseconds. The fact that the hydrogen bond lifetimes in the simulations are three orders of magnitude longer than the time scale for proton transfer on strongly hydrogen bonded systems in gas phase suggests that once either asp83 or glu22 becomes protonated, it will transfer the proton to the other residue by means of direct proton transfer (the nearest protein residues and surrounding water molecules influence the proton transfer reactions, but will not make them three order of magnitude slower than in vacuo). Thus, the proton will be shared between the residues until the hydrogen bond breaks.

Table 2
The relative fraction of simulation time in which glu22 and asp83 formed hydrogen bonds between them or with the water

Type of h-bond	Property	Run 1	Run 2	Run 3	Run 4
glu22–asp83	Fraction of simulation time	15%	61%	35%	25%
glu22–water	Fraction of simulation time	86%	48%	28%	78%
	Average number of h-bonds	1.26±0.69	ND[a]	ND[a]	1.03±0.70
asp83–water	Share of simulation time	100%	100%	100%	100%
	Average number of h-bonds	5.69±1.42	5.23±1.44	4.99±1.65	5.24±1.50

The average number of h-bonds with the water is also given. Please note that each O¯H¨O bond is listed, even if one molecule is involved in more than one bond.
[a] ND — not determined. The average number of hydrogen bonds is smaller than one, and the standard deviation is as large as the average or even larger.

3.6. Proton transfer via interconnecting water molecules in the simulations with protonated glu22

Intramolecular proton transfer may involve the transient protonation of water molecules that interconnect the donor and the acceptor, as in the enzymes bacteriorhodopsin [27,29,46,47], carbonic anhydrase [15,16] and cytochrome *c* oxidase [28]. Intermolecular proton transfer on the surface of fluorescein (a small charged molecule, which has two distinct proton binding sites) was previously measured by Mezer and colleagues [18]. MD simulations which followed those measurements revealed that the proton transfer was mediated through 4–5 interconnecting water molecules located beneath a negative Coulomb cage created by the fluorescein molecule. In order to find out whether a similar mechanism is operative between glu22 and asp83, we first checked if the residues are solvated throughout the simulations. We then tried to identify configurations in which proton transfer from glu22 to asp83 can be mediated by interconnecting water molecules.

The probability of finding hydrogen bonds between the protonated glu22 and the water and between asp83 and the water is given in Table 2, rows 2 and 3. Asp83 is hydrogen-bonded to the water throughout all the simulation times in all simulations as expected due to its negative charge. Glu22, however, is only partially hydrogen bonded with the water. The relative fraction of the simulation time, in which the protonated glu22 is hydrogen bonded to the water, varies between the four simulations, but is never close to unity. It can be as small as 28% or as large as 86% of the simulation time.

The search for configurations in which proton transfer from glu22 to asp83 could be mediated through interconnecting water molecules was performed on a trajectory which spanned 3 ns of simulation, during which time no direct hydrogen bond was located between glu22 and asp83. The analysis was performed by searching for the minimal number of water molecules that connect the donor and the acceptor in each configuration. Two oxygen atoms (OE of glu22, OD of asp83 or water oxygens) were considered as connected if the distance between them was smaller than 0.35 nm, as in [18]. It was found that the donor and the acceptor were interconnected by water molecules throughout the whole 3 ns trajectory, and that the number of interconnecting water molecules was 2.52 ± 0.89. As an example, a configuration in which the interconnecting water network is visible can be seen in Fig. 6.

In order to validate whether proton transfer between these two residues on the protein surface is probable under these conditions, let us consider our previous study, where we investigated the mechanism of proton transfer between a donor and an acceptor located some 0.6 nm apart on the same molecule (fluorescein). There, proton transfer from the donor to the acceptor (interconnected by 4–5 water molecules) was as efficient as proton transfer from the donor to the bulk. All the interconnecting water trajectories were located under the negatively charged Coloumb cage which surrounded the molecule [18]. In the study reported here, the interconnecting water molecules are located inside the negative Coulomb cage, which extends to the bulk some

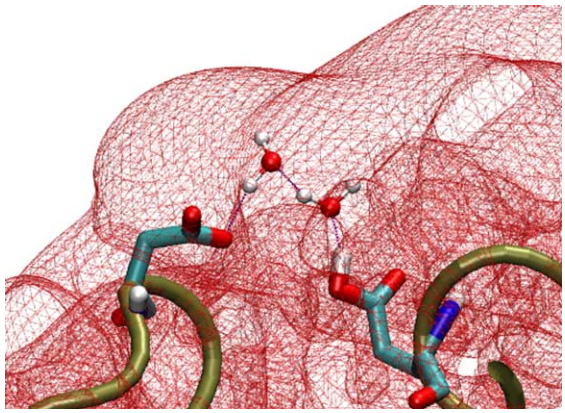

Fig. 6. A connection between the hydrogen of the protonated glu22 and the carboxylate of asp83, formed through 2 interconnecting water molecules. The negative Coloumb cage around the protein is shown in red. (For interpretation of the references to colour in this figure legend, the reader is referred to the web version of this article.)

0.4 nm from asp22 and glu83 (for example, see Fig. 6, where the negative Coloumb cage is shown in red). Therefore, solvent mediated proton transfer from glu22 to asp83 will be productive in the present case; once a proton is ejected from glu22, it has a higher chance of being transferred to asp83 than to a bulk water molecule.

3.7. Proton transfer on the protein surface: application for other systems

One of the main conclusions of our simulations is that any pair of aspartate or glutamate residues, whose carboxylate oxygens are located less than 1 nm apart, is a suitable candidate for proton transfer once one of its members becomes protonated, provided that its charge is not neutralized. This conclusion can be used to set a tool for the search of proton transferring pairs in other proteins.

Solvent-mediated proton transfer on the protein surface was evidenced in proton transferring membrane-bound proteins such as bacteriorhodopsin [5,19] and cytochrome *c* oxidase. In the latter case, the protons are transferred into the protein via two pathways, known as the K-pathway and the D-pathway. A plethora of residues on the surface of cytochrome C oxidase were suggested to be involved in the proton transfer, especially via the D-pathway (for review, see [48]). The search for residues that can be involved in the proton transfer can be refined by examining which of the aspartate, glutamate or histidine residues of the protein are located at a suitable distance to allow proton transfer between them and the entry site of the D-pathway (asp132I) or K-pathway (glu102II). Accordingly, the surface of cytochrome oxidase (taken from its crystal structure, PDB code 1M56 [49]), was searched for pairs of residues that can be involved in such proton transfer events. All aspartate, glutamate and histidine residues, whose OD atoms (in aspartate), OE atoms (glutamate) or imidazole nitrogens (histidines) were located less than 1 nm from the nearest relevant atom in the entry of the D-pathway (asp132I) or the

K-pathway (glu102II), were marked. These residues formed the first circle of possible proton donors to asp132I or glu102II. In order to examine whether there exists a second circle of possible proton donors, the same procedure was repeated, this time searching for histidine, aspartate or glutamate residues in the vicinity of the residues that belong to the first circle. For example, one of the imidazole nitrogens of his26I is located 0.313 nm from the nearest carboxylate oxygen of asp132I. Hence, the search was expanded in order to locate all relevant residues in the vicinity of his26I.

In the case of the K-pathway, only a single residue was located near the entry site (his96II, 0.716 nm). On the other hand, many such residues were identified in the D pathway; these residues and the distances between the pairs are listed in Table 3. Fig. 7 presents the residues on the surface of the cytochrome C oxidase near the entry of both pathways. The residues are presented as van der Waals spheres on the secondary structure of the protein (Fig. 7A, bottom, colored magenta and red); the network is presented in Fig. 7B. It can be seen that there are plenty of residues which can hold protons near the D-pathway. The multitude of these residues ensures that once a proton is trapped by one residue, it has a high probability to reach the channel orifice (asp132I) through a percolating network of proton collecting residues and waters.

4. Concluding remarks

In this study, we have used conventional MD simulations to demonstrate that a pair of carboxylate residues on the surface of a small protein can be found in configurations that enable proton transfer between them, despite their negative charge. Using a certain pair of nearby negative residues, it was demonstrated that direct proton transfer events through a common hydrogen bond are very probable. Likewise, solvent-mediated proton transfer events through a network of interconnecting water molecules are also expected to occur.

Table 3
The minimal distances (in nm) between possible proton transferring atoms (aspartate OD, glutamate OE and histidine ND1 or NE2) in the orifice of the cytochrome *c* oxidase D pathway

Residue 1	Residue 2	Distance
D132I	**H26I**	**0.313**
D132I	**H549I**	**0.743**
D132I	**E548I**	**0.914**
D132I	**D28I**	**0.929**
D132I	**H7III**	**0.944**
H26I	D28I	0.875
H26I	E539I	0.978
H26I	H127I	0.987
H549I	E548I	0.422
H549I	E552I	0.522
H549I	H7III	0.916
H549I	D28I	0.974
E548I	D28I	0.692
H7III	D8III	0.711
H7III	E552I	0.813

The calculations were performed using the crystal structure of Cytochrome C Oxidase From *Rhodobacter sphaeroides*, PDB code 1M56 [49]. The distances between the orifice of the D pathway (asp132I) and residues that are directly in contact with it are shown in bold letters.

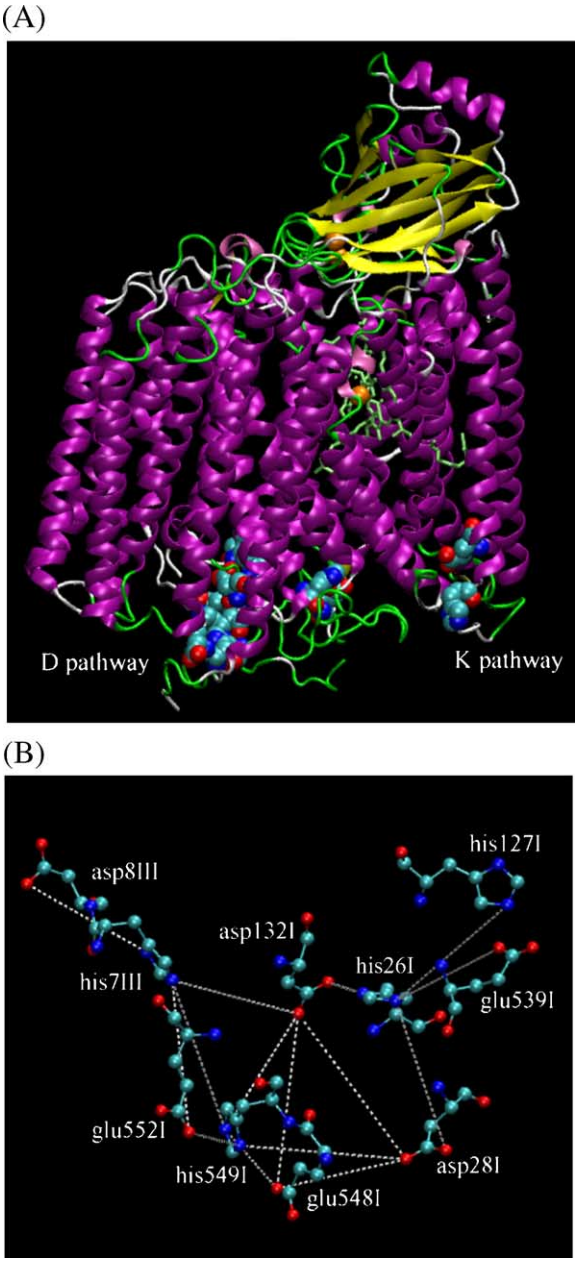

Fig. 7. (A) The entries for the proton transfer pathways in cytochrome *c* oxidase. The aspartate, glutamate and histidine residues on the surface of the cytochrome *c* oxidase near the entries of both pathways are presented as van der Waals spheres on the secondary structure of the protein. Note the abundance of residues that can hold and release protons near the entry of the D-pathway. For the distances between the residues, see Table 3. The color code is as follows: carbon atoms in magenta, nitrogen atoms in blue, oxygen atoms in red, α-helices in purple, β-sheets in yellow, random coil in green and turns in white. The locations of both pathways are indicated. (B) The interconnecting network between the residues located in the vicinity of the entry site for the D-pathway (asp132I). This entry site is located in the centre of the figure. (For interpretation of the references to colour in this figure legend, the reader is referred to the web version of this article.)

It was previously stated that pairs of carboxylic acid side chains in many proteins can share a proton [14]. In the present manuscript, this was demonstrated on the protein's surface for the first time; not on a crystal structure but throughout a simulation. This was also the first MD simulation that identified situations, in which carboxylic residues were interconnected via water molecules on the protein surface, thus enabling proton transfer between them. As this was observed on a globular protein which has no known function associated with proton transfer, we consider this as evidence for the generality of the mechanism. Thus, the surface of proteins features both ion-binding [31] and proton transferring/sharing domains that can be utilized by proteins for enzymatic catalysis, protein–solvent interactions and even for the adsorption of ligands on the protein surface [33]. From a biotechnological point of view, these features can also be applied to protein design and engineering. Furthermore, the detection of domains capable of supporting rapid proton transfer on a protein which also has ion-binding domains, supports the notion that clusters of carboxylates are the operative elements of proton collecting antennae, as in bacteriorhodopsin, cytochrome C oxidase or the photosynthetic reaction center [5,17,20,21].

Acknowledgements

This research is supported by the Israel Science Foundation (grant No 427/01-1) and the United States-Israel Binational Science Foundation (grant No 2002129). The authors would like to acknowledge the use of computer resources belonging to the Bioinformatics Unit at Tel Aviv University and the High Performance Computing Unit, a division of the Inter University Computing Center in Israel. R.F would like to acknowledge the Colton Foundation.

References

[1] N. Adir, H.L. Axelrod, P. Beroza, R.A. Isaacson, S.H. Rongey, M.Y. Okamura, G. Feher, Co-crystallization and characterization of the photosynthetic reaction center-cytochrome *c*2 complex from *Rhodobacter sphaeroides*, Biochemistry 35 (1996) 2535–2547.

[2] P. Adelroth, D.M. Mitchell, R.B. Gennis, P. Brzezinski, Factors determining electron-transfer rates in cytochrome *c* oxidase: studies of the FQ(I-391) mutant of the *Rhodobacter sphaeroides* enzyme, Biochemistry 36 (1997) 11787–11796.

[3] P. Adelroth, R.B. Gennis, P. Brzezinski, Role of the pathway through K(I-362) in proton transfer in cytochrome *c* oxidase from *R. sphaeroides*, Biochemistry 37 (1998) 2470–2476.

[4] P. Adelroth, M.L. Paddock, L.B. Sagle, G. Feher, M.Y. Okamura, Identification of the proton pathway in bacterial reaction centers: both protons associated with reduction of QB to QBH2 share a common entry point, Proc. Natl. Acad. Sci. U. S. A. 97 (2000) 13086–13091.

[5] S. Checover, Y. Marantz, E. Nachliel, M. Gutman, M. Pfeiffer, J. Tittor, D. Oesterhelt, N.A. Dencher, Dynamics of the proton transfer reaction on the cytoplasmic surface of bacteriorhodopsin, Biochemistry 40 (2001) 4281–4292.

[6] J. Teissie, M. Prats, P. Soucaille, J.F. Tocanne, Evidence for conduction of protons along the interface between water and a polar lipid monolayer, Proc. Natl. Acad. Sci. U. S. A. 82 (1985) 3217–3221.

[7] J. Heberle, J. Riesle, G. Thiedemann, D. Oesterhelt, N.A. Dencher, Proton migration along the membrane surface and retarded surface to bulk transfer, Nature 370 (1994) 379–382.

[8] D. Poulidi, M.A. Castillo-del-Rio, R. Salar, A. Thursfield, I.S. Metcalfe, Electrochemical promotion of catalysis using solid-state proton-conducting membranes, Solid State Ionics 162 (2003) 305–311.

[9] M. Iannuzzi, M. Parrinello, Proton transfer in heterocycle crystals, Phys. Rev. Lett. 9 (2004) 025901.

[10] S. Tanimura, T. Matsuoka, Proton transfer in Nafion membrane by quantum chemistry calculation, J. Polym. Sci. Polym. Phys. 42 (2004) 1905–1914.

[11] K. Brunaldi, M.A. Miranda, F. Abdulkader, R. Curi, J. Procopio, Fatty acid flip-flop and proton transport determined by short-circuit current in planar bilayers, J. Lipid Res. 46 (2005) 245–251.

[12] G. Zundel, Proton polarizability and proton transfer processes in hydrogen bonds and cation polarizability of other cation bonds. Their importance to understand molecular processes in electrochemistry and biology, Trends Phys. Chem. 3 (1992) 129–156.

[13] M.W. Flocco, S.L. Mowbray, Strange bedfellows—Interactions between acidic side-chains in proteins, J. Mol. Biol. 254 (1995) 96–105.

[14] G. Wohlfahrt, Analysis of pH-dependent elements in proteins: geometry and properties of pairs of hydrogen-bonded carboxylic acid side-chains, Proteins 58 (2005) 396–406.

[15] Q. Cui, M. Karplus, Is a "Proton Wire" concerted or stepwise? A model study of proton transfer in carbonic anhydrase, J. Chem. Phys., B 107 (2003) 1071–1078.

[16] A. Isaev, S. Scheiner, Proton conduction by a chain of water molecules in carbonic anhydrase, J. Chem. Phys., B 105 (2001) 6420–6426.

[17] M. Gutman, E. Nachliel, Time resolved dynamics of proton transfer in proteinous systems, Annu. Rev. Phys. Chem. 48 (1997) 329–356.

[18] A. Mezer, R. Friedman, O. Noivirt, E. Nachliel, M. Gutman, The mechanism of proton transfer between adjacent sites exposed to water, J. Chem. Phys., B 109 (2005) 11379–11388.

[19] S. Checover, E. Nachliel, N.A. Dencher, M. Gutman, Mechanism of proton entry into the cytoplasmic section of the proton-conducting channel of bacteriorhodopsin, Biochemistry 36 (1997) 13919–13928.

[20] Y. Marantz, E. Nachliel, A. Aagaard, P. Brzezinski, M. Gutman, The proton collecting function of the inner surface of cytochrome *c* oxidase from *Rhodobacter sphaeroides*, Proc. Natl. Acad. Sci. U. S. A. 95 (1998) 8590–8595.

[21] Y. Marantz, O.O. Einarsdottir, E. Nachliel, M. Gutman, Proton-collecting properties of bovine heart cytochrome *c* oxidase: kinetic and electrostatic analysis., Biochemistry 40 (2001) 15086–15097.

[22] M. Wikstrom, C. Ribacka, M. Molin, L. Laakkonen, M. Verkhovsky, A. Puustinen, Gating of proton and water transfer in the respiratory enzyme cytochrome *c* oxidase, Proc. Natl. Acad. Sci. U. S. A. 102 (2005) 10478–10481.

[23] D. Marx, J. Hutter, in: J. Grotendorst (Ed.), Modern Methods and Algorithms of Quantum Chemistry, NIC, Julich, 2000, pp. 301–449.

[24] A. Warshel, Computer simulations of enzyme catalysis: methods, progress, and insights, Annu. Rev. Biophys. Biomol. 32 (2003) 425–443.

[25] U.W. Schmitt, G.A. Voth, Multistate empirical valence bond model for proton transport in water, J. Phys. Chem., B 102 (1998) 5547–5551.

[26] M.A. Lill, V. Helms, Molecular dynamics simulation of proton transport with quantum mechanically derived proton hopping rates (Q-HOP MD), J. Chem. Phys. 115 (2001) 7993–8005.

[27] C. Kandt, J. Schlitter, K. Gerwert, Dynamics of water molecules in the bacteriorhodopsin trimer in explicit lipid/water environment, Biophys. J. 86 (2004) 705–717.

[28] E. Olkhova, M.C. Hutter, M.A. Lill, V. Helms, H. Michel, Dynamic water networks in cytochrome *c* oxidase from *Paracoccus denitrificans* investigated by molecular dynamics simulations, Biophys. J. 86 (2004) 1873–1889.

[29] S. Grudinin, G. Buldt, V. Gordeliy, A. Baumgaertner, Water molecules and hydrogen-bonded networks in bacteriorhodopsin—Molecular dynamics simulations of the ground state and the M-intermediate, Biophys. J. 88 (2005) 3252–3261.

[30] S.C. Agalarov, G.S. Prasad, P.M. Funke, C.D. Stout, J.R. Williamson,

Structure of the S15,S6,S18–rRNA Complex: assembly of the 30S ribosome central domain, Science 288 (2000) 107–112.
[31] R. Friedman, E. Nachliel, M. Gutman, Molecular dynamics of a protein surface: ion–residues interactions, Biophys. J. 89 (2005) 768–781.
[32] M. Lindahl, L.A. Svensson, A. Liljas, S.E. Sedelnikova, I.A. Eliseikina, N.P. Fomenkova, N. Nevskaya, S.V. Nikonov, M.B. Garber, T.A. Muranova, Crystal structure of the ribosomal protein S6 from *Thermus thermophilus*, EMBO J. 13 (1994) 1249–1254.
[33] R. Friedman, E. Nachliel, M. Gutman, Molecular dynamics simulations of the adipocyte lipid binding protein reveal a novel entry site for the ligand, Biochemistry 44 (2005) 4275–4283.
[34] E. Lindahl, B. Hess, D. van der Spoel, Gromacs 3.0: A package for molecular simulation and trajectory analysis., J. Mol. Mod. 7 (2001) 306–317.
[35] D. van Der Spoel, E. Lindahl, B. Hess, A.R. van Buuren, E. Apol, P.J. Meulenhoff, D.P. Tieleman, A.L.T.M. Sijbers, A.K. Feenstra, R. van Drunen, H.J.C. Berendsen, GROningen MAChine for molecular Simulations v. 3.2.1, Groningen. 2004.
[36] Y.P. Pan, M.A. McAllister, Characterization of low-barrier hydrogen bonds: I. Microsolvation effects. An ab initio and DFT investigation, J. Am. Chem. Soc. 119 (1997) 7561–7566.
[37] M.W. Schmidt, K.K. Baldridge, J.A. Boatz, S.T. Elbert, M.S. Gordon, J.H. Jensen, S. Koseki, N. Matsunaga, K.A. Nguyen, S. Su, T.L. Windus, M. Dupuis, J.A. Montgomery, General atomic and molecular electronic structure system, J. Comput. Chem. 14 (1993) 1347–1363.
[38] W. Kabsch, C. Sander, Dictionary of protein secondary structure: pattern recognition of hydrogen-bonded and geometrical features, Biopolymers 22 (1983) 2577–2637.
[39] W. Humphrey, A. Dalke, K. Schulten, VMD: visual molecular dynamics, J. Mol. Graph. 14 (1996) 33–38.
[40] S. Portmann, H.P. Luthi, MOLEKEL: an interactive molecular graphics tool, CHIMIA 54 (2000) 766–770.
[41] N.A. Baker, D. Sept, S. Joseph, M.J. Holst, J.A. McCammon, Electrostatics of nanosystems: application to microtubules and the ribosome, Proc. Natl. Acad. Sci. U. S. A. 98 (2001) 10037–10041.
[42] D.E. Otzen, O. Kristensen, M. Proctor, M. Oliveberg, Structural changes in the transition state of protein folding: alternative interpretations of curved Chevron plots, Biochemistry 38 (1999) 6499–6511.
[43] D.I. Svergun, S. Richard, M.H. Koch, Z. Sayers, S. Kuprin, G. Zaccai, Protein hydration in solution: experimental observation by X-ray and neutron scattering, Proc. Natl. Acad. Sci. U. S. A. 95 (1998) 2267–2272.
[44] D.A.C. Beck, D.O.V. Alonso, V. Daggett, A microscopic view of peptide and protein solvation, Biophys. Chem. 100 (2003) 221–237.
[45] M.A. Lill, V. Helms, Reaction rates for proton transfer over small barriers and connection to transition state theory, J. Chem. Phys. 115 (2001) 7985–7992.
[46] M. Weik, G. Zaccai, N.A. Dencher, D. Oesterhelt, T. Hauss, Structure and hydration of the M-state of the bacteriorhodopsin mutant D96N studied by neutron diffraction, J. Mol. Biol. 275 (1998) 625–634.
[47] A.N. Bondar, M. Elstner, S. Suhai, J.C. Smith, S. Fischer, Mechanism of primary proton transfer in bacteriorhodopsin, Structure 12 (2004) 1281–1288.
[48] P. Adelroth, P. Brzezinski, Surface-mediated proton–transfer reactions in membrane-bound proteins, Biochim. Biophys. Acta 1655 (2004) 102–115.
[49] M. Svensson-Ek, J. Abramson, G. Larsson, S. Tornroth, P. Brzezinski, S. Iwata, The X-ray crystal structures of wild-type and EQ(I–286) mutant cytochrome *c* oxidases from *Rhodobacter sphaeroides*, J. Mol. Biol. 321 (2002) 329–339.